Environ Earth Sci (2015) 73:6815–6825
DOI 10.1007/s12665-015-4157-5

THEMATIC ISSUE

Evaluation of mechanical well integrity during CO_2 underground storage

Mingxing Bai · Jianpeng Sun · Kaoping Song · Kurt M. Reinicke · Catalin Teodoriu

Received: 23 September 2014 / Accepted: 5 February 2015 / Published online: 14 February 2015

Abstract The storage of CO_2 in depleted oil and gas reservoirs, coal seams or saline aquifers is an important means considered to contribute to the mitigation of the greenhouse effect on the environment. In CO_2 underground storage projects, well integrity is a crucial factor that must be demonstrated for all wells, accessible and abandoned, affected by the injected CO_2 to ensure safety during the injection and storage of CO_2. Field experience and laboratory experiments have shown that chemical degradation due to CO_2 can affect well integrity severely only when there are existing pathways in the casing-cement-rock composite system. Therefore, the study of mechanical well integrity is of paramount significance. In this paper, analytical and numerical models are developed to assess well conditions including the micro-annulus between the cement sheath and the casing due to downhole condition changes. The parametric study shows that cement with a low Young's modulus and high Poisson ratio has smaller micro-annulus than that with a high Young's modulus and low Poisson ratio. When temperature and pressure decrease there is a potential for debonding of the interface between casing and cement.

Keywords CO_2 underground storage · Well integrity · Micro-annulus · Downhole condition changes

List of symbols

CCS	Carbon capture and sequestration
FEM	Finite element method
σ_r, σ_θ, σ_z	Radial stress, tangential, vertical stress, MPa
ε_r, ε_θ, ε_z	Radial, tangential, vertical strain (–)
σ_n	Normal stress (MPa)
τ	Shear stress (MPa)
u_s, u_c, u_f	Casing, cement and formation rock displacement (m)
μ_s, μ_c, μ_f	Poisson's ratio of casing, cement and formation (–)
E	Young's modulus (MPa)
r	Radius (m)
r_1, r_2	Inner and outer radius of the casing (m)
r_3, r_4	Outer radius of the cement and rock (m)
r_m	Average radius of the casing (m)
t_s	Casing thickness (m)
P_i	Inner pressure (MPa)
P_{c1}, P_{c2}	Contact pressure of casing/cement and cement/rock (MPa)
α	Coefficient of thermal expansion (1/°C)
$\Delta(\Delta u)$	Micro-annulus size (mm)
Δu_s, Δu_c	Casing contraction, cement contraction (mm)
ΔT	Temperature decrease (°C)

Introduction

With the industrialization in the nineteenth century, the desire for energy rose continuously resulting in a high emission of CO_2, which is considered to be one of the driving forces of climate change. One possibility of mitigating increasing emissions is to store CO_2 in the

M. Bai (✉) · J. Sun · K. Song
Department of Petroleum Engineering, Northeast Petroleum University, Daqing 163318, China
e-mail: baimingxing@hotmail.com

M. Bai · K. M. Reinicke · C. Teodoriu
Institute of Petroleum Engineering, Clausthal University of Technology, 38678 Clausthal-Zellerfeld, Germany

subsurface, e.g., depleted oil and gas reservoirs, coal seams or saline aquifers, similar to underground storage of natural gas or hydrogen (Bai et al. 2014c). Examples are the CO_2 capture and storage project in the Weyburn oil field in Canada and the ongoing project CLEAN (CO_2 Large-scale Enhanced Gas Recovery in the Altmark Natural Gas Field) in Germany (Reinicke et al. 2011; Akintunde et al. 2013). In order to increase public acceptance the injected CO_2 has to stay underground for at least 1,000 years without leaking into overlying aquifers or atmosphere (Kühn and Münch 2013).

In oil and gas fields there are normally a large number of wells that pose a great risk of anthropogenic CO_2 leakage after using the reservoir for CO_2 storage, some of which are abandoned and plugged. One of the biggest challenges for the wells in the carbon capture and storage (CCS) area is the corrosion fatigue of metals (Zhang et al. 2011). CO_2 tends to cause severe corrosion in the wellbore itself and the production facilities, in particular, if they are not designed for CO_2 service (Monne 2012; Bai et al. 2014b). The presence of galvanic corrosion, pitting and trough corrosion as well as crevice corrosion will cause local damage to the metal, which can lead to leakages through it. CO_2 is also known to disintegrate the traditional types of cement giving rise to concerns that plugging material and techniques currently in use will not suffice to seal off wells in the long term (Benge 2009; Fakhreldin et al. 2010). However, the field experience and lab experiments show that the chemical degradation can only affect well integrity severely when there are already existing pathways (Carey and Wigand 2007; IEA 2009; Bai et al. 2014a). Thus, the study of the mechanical integrity (e.g., well status after a sequence of mechanical and thermal loading in the whole life of wellbores) of the casing-cement-rock composite system is of significance for the safe, long-term containment of CO_2. These existing wells in the oil and gas field undergo pressure and temperature changes for their whole life, which result in damage to the wellbore, e.g., formation of cracks, micro-annulus, gas channeling, etc. The injected CO_2 may react with the defected cement or the casing, causing further degradation (Hou et al. 2012; De Lucia et al. 2012).

The injected CO_2 may also migrate along the defected existing wells including the CO_2 injection wells and abandoned wells. The aim of this paper is to evaluate the mechanical integrity of the existing abandoned wells prior to the injection process of CO_2 as well as the production/injection wells during the injection process of CO_2. To abandon a well, part of the casing must be cut, and then a bottom cementation is needed to shut off the formation and further plugs above it to provide additional barriers. In the near surface, the casings are cut a length of minimum 1 m for onshore wells and 5 m for offshore wells and covered by a cement plate or a steel plate. The space between the cement plugs within the casing is typically filled with drilling fluid. Before injection of CO_2 many processes, e.g., drilling process, stimulation, production, etc., could lead to failure of the wellbore. Since it is economically not worthy to open an existing abandoned well, only a simulation approach can be used to evaluate the well conditions resulting from changes in the downhole conditions.

To study mechanical integrity, the first step is to evaluate the stress distribution around a wellbore and in the annulus. For this, many researchers have developed their own theories. Thiercelin in Thiercelin et al. (1998) proposed an analytical model to describe the stress state in which the casing, cement and rock are considered to be homogeneous, isotropic and linearly elastic up to a limit value. The mechanical response of set cement under different load scenarios was studied to determine the key controlling parameters that affect well integrity. Teodoriu et al. (2010) developed an analytical model to calculate wellbore stresses and studied the casing-cement-formation interactions based on wellbore parameters. Bosma et al. (1999) used the finite element method (FEM) to study the behavior of a cement sheath under the various loads occurring during the life of a well. This model is then advanced to take more mechanisms, e.g., expansion and shrinkage, into consideration (Ravi et al. 2007). A comprehensive method called System Response Curve (SRC) was introduced firstly by Saint-Marc et al. (2008). This method replaces traditional complex simulations with wellbore component simulations and cement damage is described by various indexes.

Laboratory and modeling studies show that the principal cause of damage is the stresses induced by varying downhole conditions (Goodwin and Crook 1992; Jackson and Murphey 1993; Bosma et al. 1999; Eshiet and Sheng 2014). It is therefore important to first study the stress development due to downhole condition changes. The mechanical well conditions including the micro-annulus between the casing and the cement sheath under the influence of downhole condition changes will be determined using both analytical and numerical models. Since the focus is on the effects of downhole condition changes, for both analytical and FEM models, the initial state of stress serves as the base scenario over which the temperature and pressure-induced stresses are superimposed.

Casing-cement-rock composite system failure

Casing-cement-rock composite system failure modes

Typical failure modes of casing-cement-rock composite system include debonding of interfaces between casing and

cement or between cement sheath and rock, shear damage, radial cracking, and disking, which are shown in Fig. 1 (Bois et al. 2010). Debonding of interfaces is usually caused by shrinkage during cement hydration and a depressurization or temperature decrease inside the casing. The compressive shear failure results from a large deviatoric state of stress, or large differences of principal stresses. This difference can result from a decrease in the tangential compressive stress, which can occur during cement shrinkage. Radial cracking can be due to one of the following reasons: hydration volume reduction in the construction phase of the well, over-pressurization or temperature increase inside the casing during operation. Normally the tangential stresses are compressive. An increase pressure might turn the hoop stress into tensile. If it is in excess of a certain value, a radial crack appears. Disking occurs by axial contraction of the cement sheath when cement cannot slide at its inner or outer boundaries (Bois et al. 2010).

Downhole condition changes

A description of different scenarios of downhole condition changes is given below. Several definitions have to be explained in advance, as shown in Fig. 2. Hoop stress or tangential stress, is a normal stress in the tangential direction of a cylinder. Radial stress is a stress in directions coplanar with but perpendicular to the symmetry axis of the cylinder. These stresses determine the conditions of the casing, cement as well as the rock.

Inner pressure increase

An increase in interior pressure inside the casing due to, for instance, drilling, perforation and stimulation, can cause an increase in radial and axial stress. However, it will decrease the tangential stress and may even turn it into tensile stress. On the one hand, an increase in pressure can cause a bigger compressive stress across two interfaces (e.g., casing/cement or cement/formation) and guarantee a good well integrity. On the other hand, the tensile stress in the tangential direction can cause tensile failure if the tensile stress exceeds the tensile strength and radial cracking occurs. Therefore, the possible damage is tensile failure in the tangential direction.

Inner pressure decrease

A decrease in inner pressure due to, e.g., use of lower mud weight during drilling, can increase the tangential compressive stress. However, it will decrease the radial and axial compressive stress and even turn them into tensile stress. The interface between casing and cement is the weakest point in the composite system. So a tensile stress can possibly lead to interface failure if the tensile stress exceeds the bond strength of the two interfaces, which can be experimentally determined in the lab. In practical situations, the bond strength is very small.

Inner temperature increase

An increase in temperature (e.g., production of formation fluid) can increase the compressive stresses, e.g., σ_r, σ_θ, and σ_z shown in Fig. 2 in cylinder coordinate system, and lead to cement failure when the yield strength is exceeded. In this simulation, von Mises criteria will be used to verify the stress state.

Inner temperature decrease

A decrease of temperature due to, e.g., the injection of cold CO_2, can decrease the radial, axial and tangential stresses of the composite system. These compressive stresses may turn to tensile stresses. Because tensile strength of the interfaces is extremely low, there is potential damage to the interface or even debonding since the bond strength is small, which is assumed to be 0 in this paper.

Simulated scenarios and required data

A well in a CCS pilot area in the Altmark Natural Gas Field in North Germany, is evaluated, as a case study, using the analytical and FEM models. The model consists of

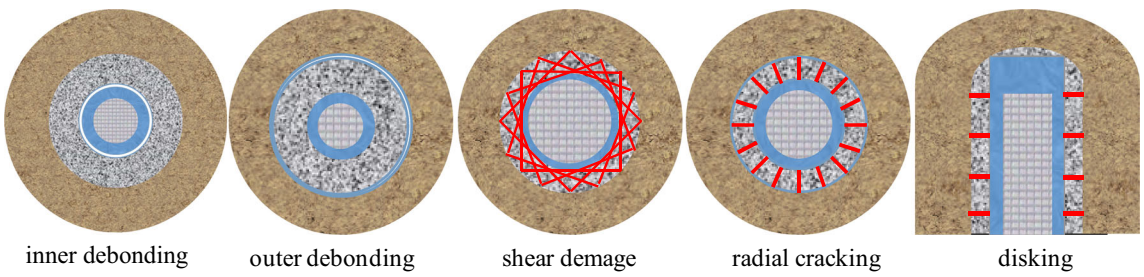

Fig. 1 Typical cement sheath damage

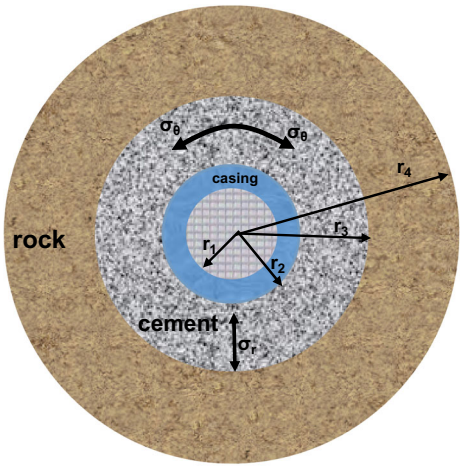

Fig. 2 Geometry of casing-cement-rock composite system

Table 1 Geometry data

Radius	r_1 (mm)	r_2 (mm)	r_3 (mm)	r_4 (mm)	r_m (mm)	t_s (mm)
Value	59.31	69.85	89.85	449.25	64.58	10.55

three concentric cylinders representing the casing, the cement sheath and part of the formation rock as shown in Fig. 2.

Input data

The geometry data and material properties selected for the model are listed in Tables 1 and 2, respectively, in which r_m represents the mean radius between inner and outer radius of the casing, and t_s represents the casing thickness.

Scenarios to be simulated

For the case study, a formation pressure (P_f) of 90 MPa and inner pressure (P_i) of 85 MPa are assumed as the base case. An inner pressure of 30 and −30 MPa (base case) was applied to the casing to represent an increased and decreased pressure, respectively. From an initial temperature T_0, the wellbore experienced two temperatures T_1 and T_2 ($T_1 \geq T_2$). A uniform temperature of 30 and −30 °C was applied to the composite system to mimic an increased and decreased temperature ($\Delta T = T_1 - T_2$), respectively. For analytical modeling, two scenarios are focused on which are temperature decrease and pressure decrease, because these two scenarios might lead to the occurrence of micro-annulus.

Since no detailed information regarding the mechanical properties of the cement sheath for most existing wellbores is available, a parametric study on linear elastic properties of cement sheath is performed. For the base case, the Young's Modulus and Poisson's Ratio (PR) for cement are 15 GPa and 0.2, respectively. Different scenarios are calculated and compared to the base scenario varying the cement properties according to Table 3. Firstly, fixing the Poisson ratio at 0.2, the Young's Modulus is changed from 5 to 25 GPa to study the influences of Young's Modulus on cement behaviors. To study the influences of Poisson ratio, the Young's Modulus is fixed and the Poisson ratio is changed from 0.1 to 0.3.

Assumptions

For simplicity several assumptions are made:

- The geometry of the casing-cement-rock composite system does not change along the interval of interest and there is no axial movement.
- Horizontal field stresses are isotropic.
- Casing, cement sheath and rock are thermo-elastic materials.
- The interface between casing and cement sheath is unbonded, and the interface between cement and rock is fully bonded. For fully bonded interface, the coincident nodes were coupled in the FEM model, to prevent the areas from slipping.
- Plane strain and axisymmetry (radial symmetric) are assumed. Axisymmetry assumes that the geometry and loading are symmetric in all directions about the axis on the solid of revolution. Plane strain assumes that the body thickness is so big that the lateral deformation is negligible.
- For the analytical model, thin-walled pipe is selected for the casing and thick-walled pipe is selected for the cement sheath and formation rock.
- For the FEM model, thick-walled pipe is selected for all the cylinders.
- The sign convention is that tensile stress is positive and compressive stress is negative.

Analytical modeling

Governing equations

Continuity equations (Geometry equations)

$$\varepsilon_r = \frac{(u+du)-u}{(r+dr)-r} = \frac{du}{dr} \tag{1}$$

$$\varepsilon_\theta = \frac{(r+u)d\theta - rd\theta}{rd\theta} = \frac{u}{r} \tag{2}$$

Table 2 Mechanical and thermal properties of materials used in the pilot area

Material	Density (kg/m^3)	Specific heat capacity [j/(kg k)]	Thermal conductivity [W/(m k)]	Thermal expansion coefficient (10^{-6} K^{-1})	Young's modulus (GPa)	Poisson ratio
Casing	7,800	1,000	45	25	210	0.26
Cement	2,300	900	0.8	12	15	0.2
Rock	2,500	900	2.4	15	21	0.17

Table 3 Variation of mechanical properties of cement

Fixed Poisson ratio		Fixed Young's modulus	
E (GPa)	Poisson ratio	E (GPa)	Poisson ratio
5	0.2	15	0.1
10			0.15
15			0.2
25			0.3

Physical equations (Hook's law)

$$\varepsilon_r = \frac{1}{E}[\sigma_r - \mu(\sigma_\theta + \sigma_z)] + \alpha\Delta T \tag{3}$$

$$\varepsilon_\theta = \frac{1}{E}[\sigma_\theta - \mu(\sigma_r + \sigma_z)] + \alpha\Delta T \tag{4}$$

$$\varepsilon_z = \frac{1}{E}[\sigma_z - \mu(\sigma_\theta + \sigma_r)] + \alpha\Delta T \tag{5}$$

Equilibrium equation

$$\frac{d\sigma_r}{dr} + \frac{\sigma_r - \sigma_\theta}{r} = 0 \tag{6}$$

where, ε_r, ε_θ, and ε_z denote radial, tangential and vertical strain, respectively. σ_r, σ_θ, and σ_z denote radial, tangential and vertical stress, respectively. u denotes displacement, and α coefficient of thermal expansion.

Stress distribution and radial displacement

The assumption of plane strain implies that the vertical strain shown in Eq. 5 is zero ($\varepsilon_z = 0$) which leads to an expression of σ_z. Inserting the expression of σ_z into Eq. 4 yields the expression ε_θ in terms of σ_θ and σ_r. Thus the radial displacement u can be derived from Eq. 2, as expressed in Eq. 7:

$$u = \frac{r}{E}\left[\sigma_\theta(1-\mu^2) - (\mu+\mu^2)\sigma_r + (1+\mu)\alpha E\Delta T\right] \tag{7}$$

In this equation, only the tangential and radial stress σ_θ and σ_r are unknown.

For the casing, the thin-walled theory is used (Teodoriu et al. 2010). At $r = r_1$,

$$\sigma_r|_{r=r_1} = P - P_{c1} \qquad \sigma_\theta|_{r=r_1} = \frac{(P_i - P_{c1})r_m}{t_s} \tag{8}$$

For the cement and formation, the thick-walled theory is used. By solving Eq. 6, Lame's equation is obtained. The radial, tangential stresses in the cement sheath are expressed as (Ugwu 2008):

$$\sigma_r = P_{c1}\frac{r_2^2}{r_3^2 - r_2^2}\left[1 - \frac{r_3^2}{r^2}\right] - P_{c2}\frac{r_3^2}{r_3^2 - r_2^2}\left[1 - \frac{r_2^2}{r^2}\right] \tag{9}$$

$$\sigma_\theta = P_{c1}\frac{r_2^2}{r_3^2 - r_2^2}\left[1 + \frac{r_3^2}{r^2}\right] - P_{c2}\frac{r_3^2}{r_3^2 - r_2^2}\left[1 + \frac{r_2^2}{r^2}\right] \tag{10}$$

where P_c is the contact pressure between two cylinders in a compound cylinder. The derivation of P_c has been performed in Ugwu (2008). They are expressed as:

$$P_{c1} = \frac{FB - KC}{DB - AK} \tag{11}$$

$$P_{c2} = \frac{C - AP_{c1}}{B} \tag{12}$$

where

$$A = \frac{r_2}{E_c}\left[(1-\mu_c^2)\left(\frac{r_2^2 + r_3^2}{r_3^2 - r_2^2}\right) + (\mu_c + \mu_c^2)\right] + \frac{r_1}{E_s}\left[\frac{r_m}{t_s}\left(1 - \mu_s^2\right) + \left(\mu_s + \mu_s^2\right)\right] \tag{13}$$

$$B = -\left[\frac{r_2}{E_c}(1-\mu_c^2)\left(\frac{2r_3^2}{r_3^2 - r_2^2}\right)\right] \tag{14}$$

$$C = \frac{P\,r_1}{E_s}\left[\frac{r_m}{t_s}(1-\mu_s^2) + (\mu_s + \mu_s^2)\right] + [(1+\mu_s)r_1\alpha_s\Delta T] - [(1+\mu_c)r_2\alpha_c\Delta T] \tag{15}$$

$$D = -\left[\frac{r_3}{E_c}(1-\mu_c^2)\left(\frac{2r_2^2}{r_3^2 - r_2^2}\right)\right] \tag{16}$$

$$K = \frac{r_3}{E_f}\left[(1-\mu_f^2)\left(\frac{r_4^2 + r_3^2}{r_4^2 - r_3^2}\right) + (\mu_f + \mu_f^2)\right] + \frac{r_3}{E_c}\left[(1-\mu_c^2)\left(\frac{r_2^2 + r_3^2}{r_3^2 - r_2^2}\right) - (\mu_c + \mu_c^2)2\right] \tag{17}$$

$$F = \left[\frac{P_f r_3}{E_f}(1-\mu_f^2)\left(\frac{2r_4^2}{r_4^2 - r_3^2}\right)\right] - [(1+\mu_f)r_3\alpha_f\Delta T] + [(1+\mu_c)r_3\alpha_c\Delta T] \tag{18}$$

where, P_{c1} and P_{c2} denote the contact pressure between the casing and the cement as well as the cement and formation, respectively.

After calculation of A, B, C, D, K, F using the basic data the contact pressure P_{c1} and P_{c2} can be obtained. The resulting radial and tangential stresses according to Eqs. 8, 9, and 10 are substituted into Eq. 7, and then the expressions of radial displacement for casing, cement and formation at radius r become:

$$u_s = \frac{r(P_i - P_{c1})}{E_s}\left[\frac{r_m}{t_s}\left(1-\mu_s^2\right) - \left(\mu_s + \mu_s^2\right)\right] + (1+\mu_s)r\alpha_s(T_1 - T_0) \quad (19)$$

$$u_c = \frac{r}{E_c}\left\{\left(1-\mu_c^2\right)\left[P_{c1}\left(\frac{r_3^2+r_2^2}{r_3^2-r_2^2}\right) - P_{c2}\left(\frac{2r_3^2}{r_3^2-r_2^2}\right)\right] + P_{c1}\left(\mu_c+\mu_c^2\right)\right\} + (1+\mu_c)r\alpha_c(T_1-T_0) \quad (20)$$

$$u_f = \frac{r}{E_f}\left\{\left(1-\mu_f^2\right)\left[P_{c2}\left(\frac{r_4^2+r_3^2}{r_4^2-r_3^2}\right) - P_f\left(\frac{2r_4^2}{r_4^2-r_3^2}\right)\right] + P_{c2}\left(\mu_f+\mu_f^2\right)\right\} + (1+\mu_f)r\alpha_f(T_1-T_0) \quad (21)$$

where, the subscripts s, c, and f denotes steel (casing), cement, and formation, respectively. T_0 denotes the initial temperature, T_1 denotes the temperature before temperature drop, and T_2 denotes the temperature after temperature drop.

Estimation of micro-annulus between the casing and the cement sheath

In order to estimate the micro-annulus size between the casing and the cement due to downhole condition changes, the interface between the casing and the cement is not assumed to be bonded because the bonding strength (adhesion force) is practically very small.

Temperature decrease

Assuming the casing-cement-formation composite system has a universal temperature drop ($\Delta T = T_2 - T_1$, and $T_1 \geq T_2$), the micro-annulus results from the different contraction capacity, resulting from different coefficient of thermal expansion, of the casing and the cement sheath, which can be expressed as:

$$\Delta(\Delta u) = |\Delta u_s - \Delta u_c| \quad (22)$$

where Δu_s and Δu_c denotes the casing contraction and cement sheath contraction, respectively. The absolute value ensures a positive value of the micro-annulus size because Δu_s and Δu_m are both negative.

Since only temperature drop is taken into consideration, the contraction of casing due to temperature drop from T_2 to T_1 can be written according to Eq. 19 as:

$$\Delta u_s = u_s(\Delta T_2) - u_s(\Delta T_1) = \frac{r_1(\Delta P_{c1})}{E_s}\left[\frac{r_m}{t_s}\left(1-\mu_s^2\right) - \left(\mu_s+\mu_s^2\right)\right] + (1+\mu_s)r_1\alpha_s\Delta T \quad (23)$$

According to Eq. 20, the contraction of cement can be written as:

$$\Delta u_c|_{r=r_2} = \frac{r_2}{E_c}\left\{\left(1-\mu_c^2\right)\left[\Delta P_{c1}\left(\frac{r_3^2+r_2^2}{r_3^2-r_2^2}\right) - \Delta P_{c2}^2\left(\frac{2r_3^2}{r_3^2-r_2^2}\right)\right] + \Delta P_{c1}\left(\mu_c+\mu_c^2\right)\right\} + (1+\mu_c)r_2\alpha_c\Delta T \quad (24)$$

where,

$$\Delta P_{c1} = P_{c1}(T_1 - T_0) - P_{c1}(T_2 - T_0) \quad (25)$$

$$\Delta P_{c2} = P_{c2}(T_1 - T_0) - P_{c2}(T_2 - T_0) \quad (26)$$

$$\Delta T = T_2 - T_1 \quad (27)$$

Obviously, the contraction of cement results from temperature drop in the cement and additional contact pressure ΔP_{c2} resulting from the contraction of outer formation rock. At $r = r_3$, the radial deformations of cement and formation have the same values because this interface is fully bonded. Thus,

$$\Delta u_c|_{r=r_3} = \Delta u_f|_{r=r_3} \quad (28)$$

According to Eqs. 20 and 21, this gives:

$$\frac{r_3}{E_c}\left\{\left(1-\mu_c^2\right)\left[-\Delta P_{c2}\left(\frac{2r_3^2}{r_3^2-r_2^2}\right)\right]\right\} + (1+\mu_c)r_3\alpha_c\Delta T = \frac{r_3}{E_f}\left\{\left(1-\mu_f^2\right)\left[\Delta P_{c2}\left(\frac{r_4^2+r_3^2}{r_4^2-r_3^2}\right)\right] + P_{c2}\left(\mu_f+\mu_f^2\right)\right\} + (1+\mu_f)r_3\alpha_f\Delta T \quad (29)$$

Thus,

$$\Delta P_{c2} = \left\{[(1+\mu_c)\alpha_c\Delta T] - [(1+\mu_f)\alpha_f\Delta T]\right\} \Big/ \frac{1}{E_f}\left\{\left[\left(1-\mu_f^2\right)\left(\frac{r_4^2+r_3^2}{r_4^2-r_3^2}\right) + \left(\mu_f+\mu_f^2\right)\right] + \frac{1}{E_c}\left[\left(1-\mu_c^2\right)\left(\frac{r_3^2+r_2^2}{r_3^2-r_2^2}\right) - \left(\mu_c+\mu_c^2\right)\right]\right\} \quad (30)$$

Substituting Eqs. 30, 24 and 23 into Eq. 22 yields an expression of the micro-annulus between the casing and the cement due to temperature drop.

Pressure decrease

After the pressure decrease the casing will shrink. In case the initial state of cement sheath behaves plastic, which means the cement sheath cannot follow the casing, a micro-annulus occurs. If the deformation of cement sheath is ignored, Eq. 33 can be used to roughly estimate the micro-annulus size between casing and cement owing to the inner pressure drop.

$$u_s = \varepsilon_\theta \times r_2 = \frac{r_2(P_i - P_{c1})}{E_s}\left[\frac{r_m}{t_s}(1-\mu_s^2) - (\mu_s + \mu_s^2)\right] + (1+\mu_s) r_2 \alpha_s \Delta T \quad (31)$$

$$u_s' = \varepsilon_\theta \times r_2 = \frac{r_2(P_i + \Delta P - P_{c1})}{E_s}\left[\frac{r_m}{t_s}(1-\mu_s^2) - (\mu_s + \mu_s^2)\right] + (1+\mu_s) r_2 \alpha_s \Delta T \quad (32)$$

$$\Delta u_s = u_s - u_s' = \frac{r_2(-\Delta P)}{E_s}\left[\frac{r_m}{t_s}(1-\mu_s^2) - (\mu_s + \mu_s^2)\right] \quad (33)$$

Numerical simulation using finite element method

For a detailed simulation of mechanical integrity, the finite element method (FEM) is used. FEM is applied to a system by spatially discretizing the system and solving the FEM mathematics simultaneously across the geometry. In the FEM, the casing, cement and rock are divided into a finite number of elements so that the governing equations can be solved. When analyzed, each element must satisfy the constraints set by the user.

An advantage of axisymmetry (radial symmetry) is that it allows a portion of the solid cylinder to be modeled without losing accuracy. It is therefore sufficiently accurate to model only a quarter of the geometry in this case. It is usually assumed that the radius of model is at least 10 times that of wellbore radius so that the far field stresses in the formation remain unchanged from the initial value, as shown in Fig. 3 (Ravi et al. 2007). A 2-D, eight-node, structural solid, quadrilateral, higher-order element PLANE 183 was selected. Contact elements were used to model the connection between the casing and the cement. The inner surface of the cement is defined as the target surface and outer surface of the production pipe as the contact surface.

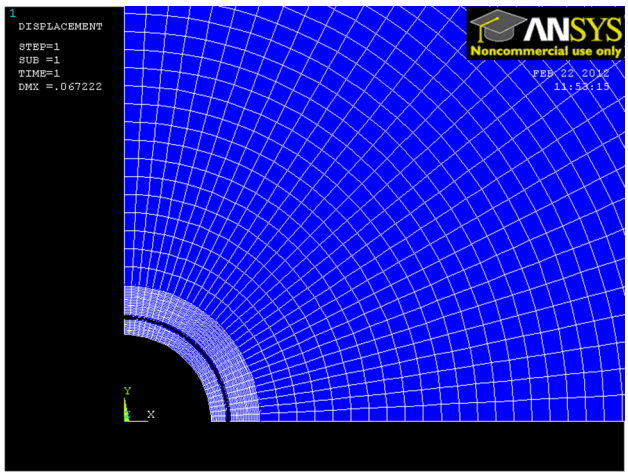

Fig. 3 Model geometry in the FEM simulator ANSYS

The casing was modeled with 40 × 4 quadrilateral elements, the cement with 40 × 10 of such elements and the formation by 40 × 30 elements, because only the influence of the downhole condition changes on well integrity, or specifically, the pressure and temperature variations were considered. The initial stresses in the composite system were not considered and there was no force between casing and cement or cement and rock.

Simulation results

Inner pressure increase

The additional tangential stresses and von Mises stresses in the casing due to pressure increase are shown in Figs. 4 and 5, respectively. Both approaches show that increasing Young's modulus will lead to increasing additional stress while increasing Poisson ratio will lead to decreasing additional stress, and increasing Young's modulus will lead to decreasing additional von Mises stress while decreasing Poisson ratio will lead to decreasing additional stress.

Inner pressure decrease

Since a pressure decrease might lead to interface debonding, the point of interest is the radial stresses at the interfaces. The radial stresses and the resulting micro-annulus at the two interfaces are shown in Figs. 6 and 7, respectively. Both analytical and numerical approaches show that the tensile stress at the first interface (casing/cement) is bigger than that at the second one, and increasing Young's modulus will increase the tensile radial stress while increasing Poisson ratio will decrease the tensile radial stress at the

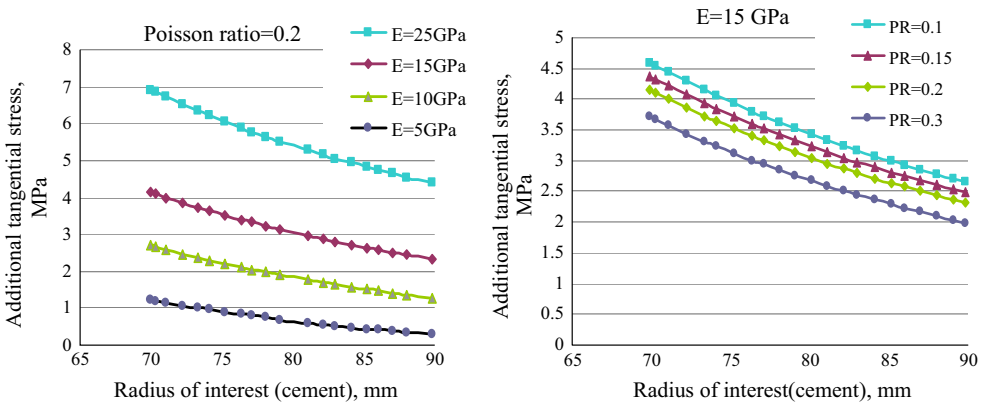

Fig. 4 Additional tangential stress in the cement sheath due to pressure increase inside the casing

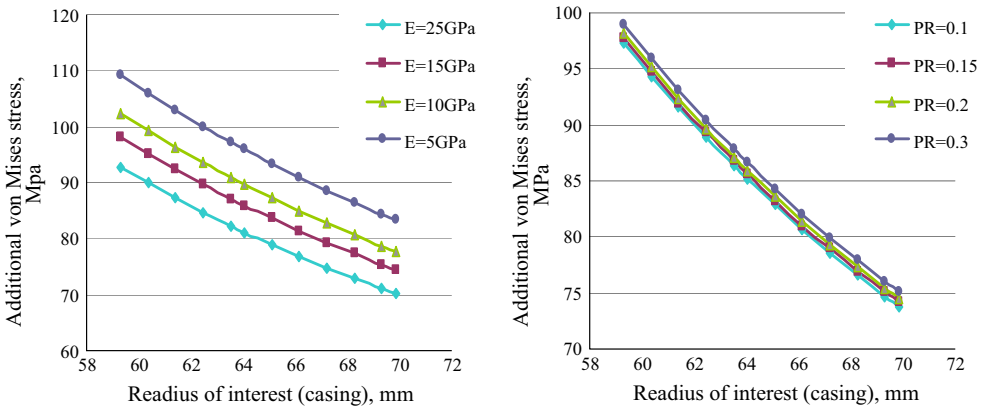

Fig. 5 Von Mises stress in the casing due to pressure increase inside the casing

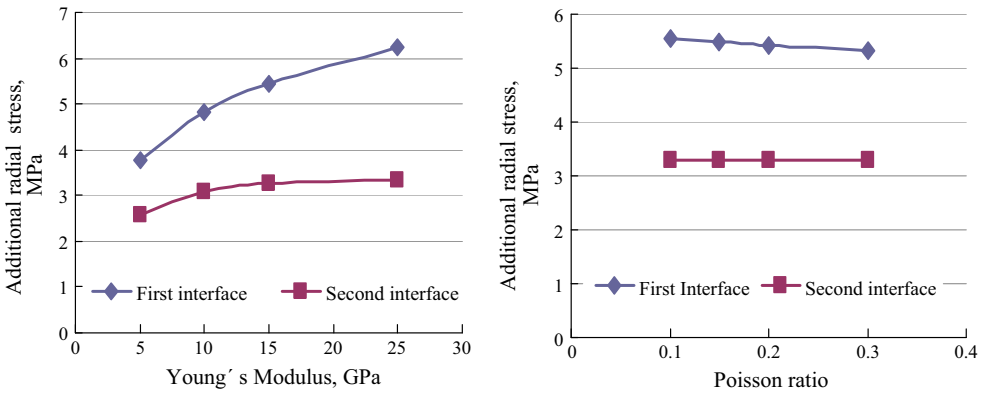

Fig. 6 Additional radial stress at the interfaces due to pressure drop

first interface slightly. A higher pressure drop will cause a bigger micro-annulus.

Temperature increase

Since an increased temperature might lead to failure after the yield point is exceeded, the von Mises stresses across the casing and cement sheath are calculated and verified. The results are shown in Fig. 8 for the simulated scenarios. It can be seen that increasing Young's modulus will increase the von Mises stress in the casing and cement owing to the temperature increase, but Poisson ratio does not have much impact.

Temperature decrease

For temperature decrease the radial stresses and the resulting micro-annulus at the two interfaces are shown in Figs. 9 and 10, respectively. Both analytical and numerical simulation show that the tensile stress at the first interface

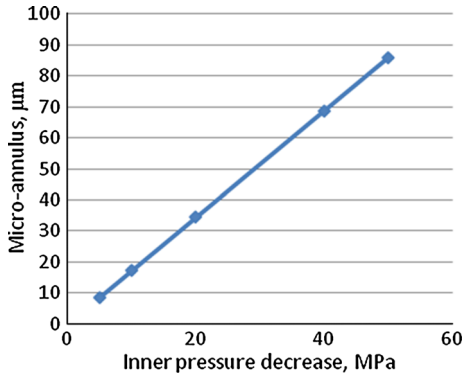

Fig. 7 Micro-annulus between casing and cement sheath due to pressure drop inside the casing

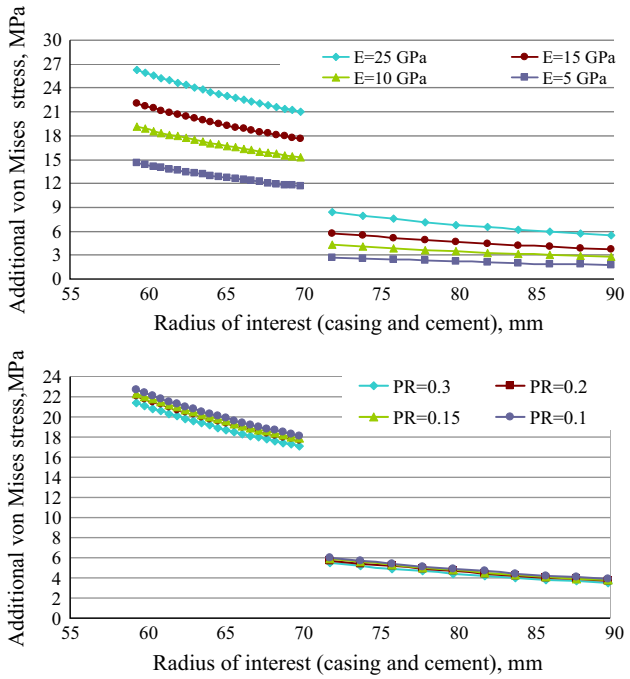

Fig. 8 Additional von Mises stress in the casing and cement due to temperature increase inside the casing

is bigger than that at the second one, and increasing Young's modulus will increase the tensile radial stress while increasing Poisson ratio will decrease the tensile radial stress slightly.

Comparison of analytical and numerical simulation results

Figure 11 shows the von Mises stress comparison using the analytical and FEM models. It can be seen that the two lines are very similar with an average error of 1 %. Figure 12 shows the comparison of the different micro-annulus size using analytical and FEM techniques under conditions of pressure and temperature decrease. For pressure drops, the two lines have a maximum error of 3 %, and for temperature drops, the two lines have a maximum error of 5 %.

Discussion

Four scenarios, which are pressure increase, pressure decrease, temperature increase and temperature decrease, have been simulated.

For pressure increase inside the casing, it can be seen that the highest tangential stress is at the casing/cement interface while the lowest is at the cement/rock interface. The stress at the cement/formation interface is less tensile or even compressive, owing to the mechanical support from the formation rock. Under the same conditions, the interior of the casing has the greatest von Mises stress. If it exceeds the yield strength, the casing will fail.

For pressure decrease, the additional radial stress is the point of interest. The additional radial stress is added to the original compressive stress, and if it exceeds the bond strength of the interface, which is assumed zero in this paper, debonding occurs. Since debonding often occurs at the casing/cement interface, a micro-annulus is assumed to be

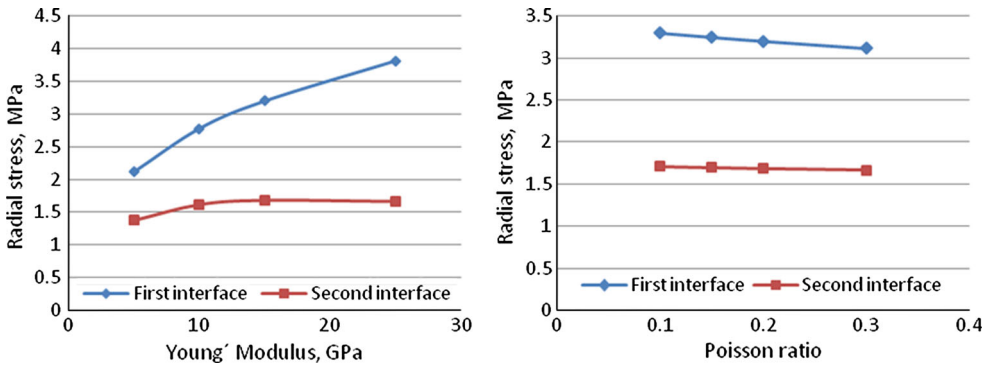

Fig. 9 Additional radial stress at interfaces due to temperature drop inside the casing

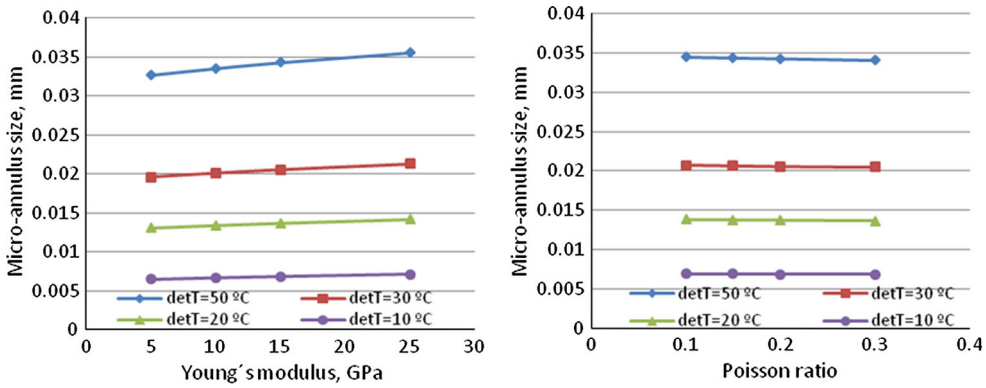

Fig. 10 Micro-annulus size due to temperature drop inside the casing

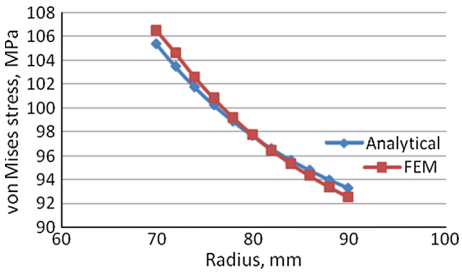

Fig. 11 Von Mises stress comparison using analytical and numerical models

created here (Nelson and Guillot 2006). Then a decreased pressure will make the casing shrink inwardly and a gap appears providing that the cement sheath behaves plastic.

For temperature increase, the von Mises stress is the point of interest. Under the same conditions, the casing has a much bigger von Mises stress than the cement and the interior of the casing has the largest one. Cement failure will occur when the yield strength is exceeded.

For temperature decrease, radial stresses at interfaces are point of interest. A micro-annulus will occur due to the different contraction capacity (coefficient of thermal expansion) of casing and cement resulting from decreased temperature. Obviously increasing Young's modulus can lead to an increase in the micro-annulus size and Poisson ratio does not have much impact. A greater temperature drop will apparently increase the micro-annulus size.

The different results from the analytical and FEM simulation, shown in Figs. 11 and 12, are caused by many reasons in addition to the different algorithms. For instance, the thin-walled cylinder implies a single average value for the stresses across the casing diameter but the FEM would do the same calculations for different elements across the casing. Comparison between analytical and numerical models reveals that the analytical models can generate reasonable results given the uncertainty of the input parameters.

Conclusions

An analytical model and a numerical model were used to evaluate the mechanical integrity of the wellbore, e.g., stress distribution, micro-annulus development between the casing and the cement sheath and so on. Given the uncertainties of the system, the analytical model can be applied to predict the well integrity response due to the downhole condition changes during the life of the wellbore and provide a characterization of the defects, which are used for permeability estimation. The results show that the cement with low Young's modulus and high Poisson ratio

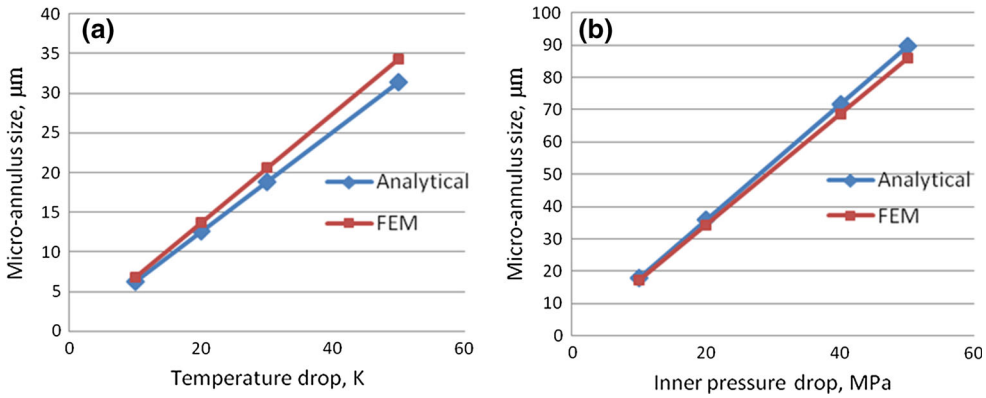

Fig. 12 Micro-annulus size for **a** temperature drop and **b** pressure drop

performs better, viz., leading to smaller micro-annulus, than then the cement with high Young's modulus and low Poisson ratio. For decreases in temperature and pressure, there is a potential debonding of the casing and the cement sheath.

Comparison between analytical and numerical models reveals that the analytical models are relatively simple and they can generate reasonable results given the uncertainty of the input parameters. In case of more complicated and practical situations considering anisotropy and differential horizontal stresses, or where time can be implied, for example, dynamic and cyclic loading and stepwise temperature variation and so on, the FEM model can be used.

Debonding of interfaces and the resulting fluid pathway has been estimated through the mechanical integrity evaluation. This can be used to calculate the permeability of the pathway. With coupled chemical simulation cement degradation might be accessed, and long-term performance of the wellbore in terms of leakage rates of CO_2 can be evaluated.

Acknowledgments This work was financially supported by the National Natural Science Foundation of China (Grant No. 51304049). Furthermore the authors would like to thank all members of the research team.

References

Akintunde OM, Knapp C, Knapp J (2013) Petrophysical charaterization of the South Georgia Rift Basin for supercritical CO_2 storage: a preliminary assessment. Environ Earth Sci 70(7):2971–2985

Bai M (2014) Risk assessment for CO_2 leakage along abandoned wells using a monte carlo simulation in a CO_2 sequestration site. J Pet Sci Technol 32:1191–1200

Bai M, Reinicke KM, Song K, Li Y, Sun J (2014a) Relative permeability model and CO_2 leakage through abandoned wells during CO_2 underground storage. Oil Gas Eur Mag 40(3):161–165

Bai M, Song K, Li Y, Sun J, Reinicke KM (2014b) Development of a novel method to evaluate well integrity during CO_2 underground storage. SPE Journal, SPE 173000

Bai M, Song K, Sun Y, He M, Li Y, Sun J (2014c) An overview of hydrogen underground storage technology and prospects in China. J Pet Sci Eng 124:132–136

Benge G (2009) Improving wellbore seal integrity in CO_2 injection wells. SPE 119267, SPE/IADC Drilling Conference and Exhibition, Amsterdam, The Netherlands, Mar 17–19, 2009

Bois A-P, Garnier A, Galdiolo G, Laudet J-B (2010) Use of a mechanistic model to forecast cement-sheath integrity for CO_2 storage. SPE 139668, SPE International Conference on CO_2 capture, storage, and utilization, New Orleans, Nov 10–12

Bosma MGR, Ravi K, van Driel W, Schreppers J (1999) Design approach to sealant selection for the life of the well. SPE 56536 presented at the 1999 Annual Technical Conference and Exhibition, Houston, Oct 3–6

Carey JW, Wigand M (2007) Analysis and performance of oil well cement with 30 years of CO_2 exposure from the SACROC Unit, West Texas, USA. Intl J Greenh Gas Control 1:75–85

De Lucia M, Bauer S, Beyer C, Kuhn M, Nowak T, Pudlo D, Reitenbach V, Stadler S (2012) Modeling CO_2-induced fluid-rock interactions in the Altensalzwedel gas reservoir. Part I: from experimental data to a reference geochemical model. Environ Earth Sci 67(2):563–572

Eshiet K, Sheng Y (2014) Investigation of geomechanical responses of reservoirs induced by carbon dioxide storage. Environ Earth Sci 71(9):3999–4020

Fakhreldin Y, Al-Sharji H, Ruwehy AM, Saadi K, Taoutaou S, Al-Kalbani S (2010) Advanced cement system for acid gas injection wells. SPE 132345, SPE Asia Pacific Oil and Gas Conference and Exhibition, Queensland, Australia, Oct 18–20, 2010

Goodwin KJ, Crook RJ (1992) Cement sheath stress failure. SPEDE, 291–296, Dec 1992

Hou ZM, Gou Y, Taron J, Gorke UJ, Kolditz O (2012) Thermo-hydro-mechanical modeling of carbon dioxide injection for enhanced gas-recovery (CO_2-EGR): a benchmarking study for code comparison. Environ Earth Sci 67(2):549–561

IEA Greenhouse Gas R&D Program (2009) Long term integrity of CO_2 storage–well abandonment report 2009/08

Jackson PB, Murphey CE (1993) Effect of casing pressure on gas flow through a sheath of set cement. SPE 25698 presented at the SPE/IADC Drilling Conference, Amsterdam, Feb 23–25

Kühn M, Münch U (ed) (2013) CLEAN (CO_2 large-scale enhanced recovery in the Altmark natural gas field)-GEOTECHNOLOGIEN Science Report No. 19. Springer-Verlag. ISBN: 97836 42316760

Monne JJ (2012) The Lacq CCS Pilot, a First. SPE-157157-MS presented at International Conference on health, safety and environment in oil and gas exploration and production, Perth, Australia, Sep 11–13

Nelson EB, Guillot D (eds) (2006) Well cementing. Schlumberger Educational Services, Sugar Land

Ravi K, McMechan DE, Reddy BR, Crook R (2007) A comparative study of mechanical properties of density-reduced cement compositions. SPE 90068, presented at the 2004 SPE Annual Technical Conference and Exhibition, Houston, Sep 26–29

Reinicke KM, Bai M, Fichter C, Weinlich FH (2011) Leckagerisiko von Bohrungen unter Einfluss von CO_2: Von den FEPs bis zu den Szenarien. DGMK/ÖGEW–Frühjahrstagung 2011, Celle, 11/12, April 2011

Reinsch T, Henninges J, Asmundsson R (2013) Thermal, mechanical and chemical influences on the performance of optical fibres for distributed temperature sensing in a hot geothermal well. Environ Earth Sci 70(8):3465–3480

Saint-Marc J, Garnier A, Bois A (2008) Initial state of stress: the key to achieving long-term cement-sheath integrity. SPE 116651 presented at the SPE Annual Technical Conference and Exhibition, Denver, Colorado, Sep 21–24

Teodoriu C, Ugwu I, Schubert J (2010) Estimation of casing-cement-formation interaction using a new analytical model. SPE 131335, SPE EUROPEC/EAGE Annual Conference and Exhibition, Barcelona, Spain, Jun 14–17

Thiercelin MJ, Dargaud B, Baret JF, Rodriguez WJ (1998) Cement design based on cement mechanical response. SPEDC, 266–273, Dec 1998

Ugwu IO (2008) Cement fatigue and HPHT well integrity with application to life of well prediction. Master Thesis, Clausthal University of Technology

Zhang Y, Gao K, Schmitt G (2011) Inhibition of steel corrosion under aqueous supercritical CO_2 conditions. NACE CORROSION, Houston, Texas, Mar 13–17